Journal of Rajasthan Academy of Physical Sciences
ISSN: 0972-6306; URL: http://raops.org.in
Vol.24, No.1&2, January-June, 2025, 1-20

EFFECT OF INTERNAL HEAT SOURCE AND ROTATION ON THE ONSET OF DOUBLE-DIFFUSIVE NANOFLUID CONVECTION IN A SPARSELY DISTRIBUTED POROUS MEDIUM

Harjinder Singh[1], **Chitresh Kumari**[2], **Kaka Ram**[3],
Ananaya Sharma[4] and **Jyoti Prakash**[5]
[1]Department of Mathematics, Kanwar Durga Chand Govt. Degree College, Jaisinghpur, Kangra-176095, Himachal Pradesh, India.
[2]Department of Mathematics and Statistics, Himachal Pradesh University, Summerhill, Shimla-171005, Himachal Pradesh, India.
[3]Govt. Senior Secondary School Devdhar, Teh. Chachiot, Distt. Mandi-175029, Himachal Pradesh, India.
[4,5]Department of Computer Science Engineering, UIT, Himachal Pradesh University, Shimla-171005, Himachal Pradesh, India.
Email: jpsmaths67@gmail.com[1]

Abstract: In the present paper, the effect of internal heat source on the onset of double-diffusive convection in a rotating nanofluid layer saturating a sparsely distributed porous medium has been investigated using Darcy-Brinkman model. A linear stability analysis has been carried out for the case of free boundaries. Expressions for thermal Darcy-Rayleigh numbers for stationary and oscillatory convection are determined numerically and valid approximations are also made in the complex equations for oscillatory convection to get useful results. The dual impact of the Darcy number on the fluid system for stationary convection is analyzed numerically and predicted graphically. It is also shown that the parameters such as Rotation, Dufour and Soret have stabilizing influence, whereas the nanoparticle concentration Rayleigh number has a destabilizing effect on the onset of stationary convection.

Keywords: Nanofluid, Internal heat source, Rotation, Porous medium, Darcy-Brinkman Model.

Mathematics Subject Classification 76E06, 76E07, 76S05

1. Introduction

The common heat transfer fluids, like water or tri-ethylene glycols with suspended ultrafine solid nanoparticles having dimension from 1 to 100nm are called as Nanofluids. The term ‘Nanofluid’ was, first of all, used by Choi [13]. The presence of these suspended nanoparticles increases the thermophysical properties such as thermal conductivity, thermal diffusivity, viscosity and convective heat transfer coefficients compared to those of base fluids [38]. Due to the property of very high thermal conductivity, the nanofluids are used as great coolants and will also act as more effective heat exchangers in chemical production industries, power stations, transportation industry, nuclear reactors, transportation industry, micro-electromechanical systems (MEMS), electronics and instrumentation and biomedical applications (nano-drug delivery, cancer therapeutics, cryopreservation) (Khanafer et al. [21] and; Khaled and Vafai [18]).

The onset of convection in a horizontal fluid layer heated from below, known as Benard problem, has extensively been studied. For the detailed knowledge of the Benard problem one may refer to Chandrasekhar [11]. The convection in Nanofluids has also been extensively studied for last few decades. Buongiorno [9] was the first who studied convective heat transport in nanofluids. Based upon his findings Tzou [36] and Dhananjay et al. [16] studied the Rayleigh-Benard problem for nanofluids and found that regular fluids are more stable than nanofluids. For more studies on the topic of Rayleigh-Benard convection in nanofluids one may refer to Nield and Kuznetsov [28,29], Bhadauria and Agarwal [6], Khalid et al. [19] and Kiran and Manjula [22].

Double-Diffusive convection, more specifically known as thermohaline or thermosolutal convection has attracted considerable interest due to its wide range of applications in oceanography, earth's atmosphere, stellar convection, electrochemistry, prediction of groundwater movements in aquifers, in the energy extraction process from geothermal reservoirs, in nuclear engineering, etc. (Huppert and Turner [17], Malashetty et al. [26]). For the excellent review of the topic, one may be referred to Turner [35] and Radko [33]. Recently, double diffusive convection has also been investigated when the base fluid of the nanofluid is itself a binary fluid such as salty water. Kuznetsov and Nield [24], Nield and Kuznetsov [30] studied the double-diffusion convection in a horizontal nanofluid layer in porous and non-porous medium, respectively, by incorporating the effects of Brownian motion and thermophoresis. Aggrawal et al. [1] studied non-linear convective transport in a binary nanofluid saturated porous medium. Yadav et al. [40] analysed the effect of thermal conductivity and variable viscosity on the stability of double diffusive convection in a nanofluid saturated porous layer. Sharma and Gupta [34] studied double diffusive convection in a horizontal nanofluid layer in porous medium in the presence of uniform vertical rotation. Chamkha et al. [10] studied the mixed convection in a porous gamma-shaped nanofluid layer. Umavathi and Beg [37] investigated the double diffusive convection in a non-newtonian nanofluid saturated porous layer. Pundir et al. [32] investigated the stability of hybrid nanofluid layer in the presence of solute gradient when heated from below.

There are many practical situations like nuclear reactions, petroleum production, food engineering, electrical equipments, oil extractions, crystal growth, astrophysics, thermal ignition, geophysics, nuclear energy, fire and combustion studies, and storage of radioactive materials, etc. wherein a porous material or any reacting material undergoes a weak exothermic reaction and heat is being generated internally through radioactive decay or through chemical reaction. The subsequent study on internal heat generation on the onset of convection in porous and non-porous medium has attracted the attention of many researchers. Chowdhury et al. [14] studied finite element analysis of double-diffusive natural convection in a porous triangular enclosure filled with Al_2O_3-water nanofluid in presence of heat generation. Bhattacharyya and Jena [8] investigated the thermal instability of a horizontal layer of micropolar fluid with heat source. Char and Chiang [12] studied stability analysis of Benard-Marangoni convection in fluids with internal heat generation. Bhadauria et al. [7] and concluded that internal heat source destabilizes the system. Awasthi et al. [4] studied the effect of this internal heat source on the onset of triply diffusive convection in a Maxwell fluid saturated porous layer. The influence of uniform internal heat generation on the onset of convection in a horizontal nanofluid layer is studied by Yadav et al. [40, 41] and Nield and Kuznetsov [28] and predicted its destabilizing effect on the system. The effect of internal heat source on the onset of double-diffusive convection in a rotating nanofluid layer with feedback control strategy is investigated by Khalid et al. [20]. Bhadauria and Srivastava [5] investigated the combined effect of internal heating and through-flow in a nanofluid saturated porous medium under local thermal nonequilibrium. Recently, Devi et al. [15] investigated internal heat source effects on thermosolutal convection of casson nanofluids embedded by Darcy-Brinkman model. For more studies in the field of internal heat generation and flow through porous medium. One may refer to Prakash and Bala [31], Ali et al. [3], Akhila et al. [2] and Kumari et al. [23].

The aim of the paper is to examine the combined effects of rotation and internal heat source on the onset of double-diffusive nanofluid convection in porous medium using Darcy-Brinkman model. The effects of physical parameters, such as, nanoparticles, Taylor number, internal Rayleigh number, solute Rayleigh number, Darcy number and nanoparticle Rayleigh number on the stability of the system are predicted numerically using MATHEMATICA and presented graphically.

2. Mathematical formulation of the problem

Consider an infinite horizontal layer of a viscous finitely heat conducting incompressible nanofluid of thickness d, saturating a sparsely distributed porous medium which is heated and soluted from below. The fluid layer is statically confined between the horizontal boundaries $z = 0$ and $z = d$ which are respectively maintained at uniform temperatures T_0 and $T_1(< T_0)$, concentrations C_0 and $C_1(< C_0)$ and nanoparticle volume fraction φ_0 and $\varphi_1(> \varphi_0)$. The nanofluid layer rotates about the vertical axis at a constant angular velocity $\boldsymbol{\Omega}(0,0,\Omega)$ and subjected to a uniform internal heat source G_0. It is further assumed that porous medium is a constant porosity medium and the Darcy-Brinkman Model has been used to investigate the Double-Diffusive Nanofluid convection in a sparsely distributed porous medium (Fig. 1).

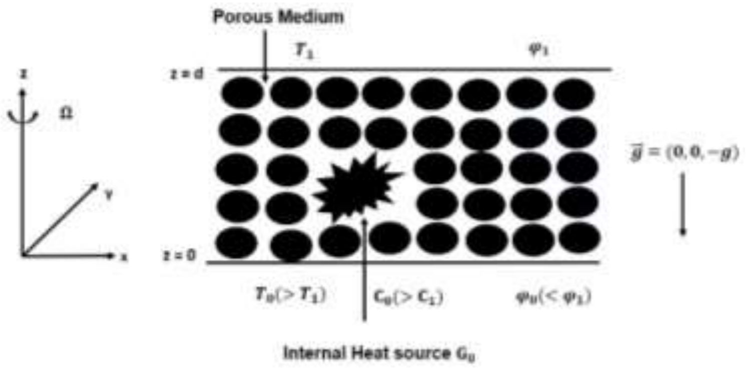

Fig. 1: Geometrical configuration of the problem

The basic equations governing the motion of nanofluid for the above model are given by (Yadav et al. [39], Nield and Kuznetsov [27,28].

$$\nabla.\boldsymbol{q}_D = 0, \qquad (1)$$

$$\frac{\rho}{\epsilon}\frac{\partial \boldsymbol{q}_D}{\partial t} = -\nabla p + \bar{\mu}\,\nabla^2\boldsymbol{q}_D - \frac{\mu}{k_1}\boldsymbol{q}_D + [\varphi\rho_P + (1-\varphi)\rho\{1-\alpha_T(T-T_1) - \alpha_C(C - C_1)\}]\boldsymbol{g} + \frac{2\rho}{\epsilon}(\boldsymbol{q}_D \times \boldsymbol{\Omega}), \qquad (2)$$

$$(\rho c)_m\frac{\partial T}{\partial t} + (\rho c)_f\boldsymbol{q}_D.\nabla T = K_m\nabla^2 T + \epsilon(\rho c)_P\left[D_B\nabla\varphi.\nabla T + D_T\frac{\nabla T.\nabla T}{T_1}\right] + (\rho c)_f D_{TC}\nabla^2 C + G_0(T-T_1), \qquad (3)$$

$$\frac{\partial C}{\partial t} + \frac{1}{\epsilon}\boldsymbol{q}_D.\nabla C = D_S\nabla^2 C + D_{CT}\nabla^2 T, \qquad (4)$$

$$\frac{\partial \varphi}{\partial t} + \frac{1}{\epsilon}\boldsymbol{q}_D.\nabla\varphi = D_B\nabla^2\varphi + \frac{D_T}{T_1}\nabla^2 T, \qquad (5)$$

where $\boldsymbol{q}_D = (u, v, w)$, t, p, ρ, ϵ, μ, $\bar{\mu}$, k_1, c, $\boldsymbol{g}\,(0, 0-g)$ denote respectively the nanofluid velocity, time, pressure, nanofluid density, porosity of the medium, fluid viscosity, medium effective viscosity, permeability of porous medium, fluid specific heat and acceleration due to gravity. Further, T is the temperature, C is the solute concentration, φ is the nanoparticle volume fraction, α_T is the thermal volumetric expansion coefficient, α_C is the analogous solute coefficient, ρ_m is the medium density, ρ_P is the nanoparticle density, c_m is the medium specific heat, c_P is the nanoparticle specific heat, K_m is the thermal conductivity of the porous medium, $(\rho c)_f$ is the heat capacity of nanofluid, $(\rho c)_m$ is the effective heat capacity of porous medium, D_B is the Brownian diffusion coefficient, D_T is the thermophoretic diffusion coefficient, D_S is the diffusivity of solute, D_{TC} is the diffusivity of Dufour type and D_{CT} is the diffusivity of Soret type.

The boundary conditions for the velocity, the temperature, the solutal concentration and the volumetric fraction of the nanoparticle are given as

$$w = 0, T = T_0, C = C_0, \varphi = \varphi_0 \text{ at } z = 0, \qquad (6)$$

$w = 0, T = T_1, C = C_1, \varphi = \varphi_1$ at $z = d$. (7)

Let us introduce dimensionless variables as

$(x^*, y^*, z^*) = (x, y, z)/d,\ t^* = t\kappa_T/\gamma d^2,\ \boldsymbol{q}^* = \boldsymbol{q}_D d/\kappa_T,\ p^* = pk_1/\mu\kappa_T\ ,\ T^* = \frac{T-T_1}{T_0-T_1}\ ,$
$C^* = \frac{C-C_1}{C_0-C_1}, \varphi^* = \frac{\varphi-\varphi_0}{\varphi_1-\varphi_0}\ ,$ (8)

where $\kappa_T = \frac{K_m}{(\rho c)_f}$ is the thermal diffusivity, $\gamma = \frac{(\rho c)_m}{(\rho c)_f}$ is the heat capacity ratio and the superscript '*' denotes the dimensionless variable.

Substituting Eq. (8) into Eqs. (1) - (5), we obtain the following nondimensional equations (dropping the asterisk '*' for simplicity)

$\nabla.\boldsymbol{q} = 0,$ (9)

$\frac{D_a}{P_r}\frac{\partial \boldsymbol{q}}{\partial t} = -\nabla p + D_a\nabla^2\boldsymbol{q} - \boldsymbol{q} - R_m\hat{k} + R_aT\hat{k} + \frac{R_s}{\tau_s}C\hat{k} - R_n\varphi\hat{k} + \sqrt{T_a}(\boldsymbol{q}\times\hat{k}),$ (10)

$\frac{\partial T}{\partial t} + \boldsymbol{q}.\nabla T = \nabla^2\mathrm{T} + \frac{N_B}{\tau_n}\nabla\varphi.\nabla T + \frac{N_AN_B}{\tau_n}\ \nabla T.\nabla T + N_{TC}\nabla^2\mathrm{C} + R_iT,$ (11)

$\frac{1}{\gamma}\frac{\partial C}{\partial t} + \frac{1}{\epsilon}\boldsymbol{q}.\nabla C = \frac{1}{\tau_s}\nabla^2\mathrm{C} + N_{CT}\nabla^2\mathrm{T},$ (12)

$\frac{1}{\gamma}\frac{\partial \varphi}{\partial t} + \frac{1}{\epsilon}\boldsymbol{q}.\nabla\varphi = \frac{1}{\tau_n}\nabla^2\varphi + \frac{\mathrm{N_A}}{\tau_\mathrm{n}}\nabla^2\mathrm{T},$ (13)

where $\boldsymbol{q} = (u, v, w)$ is the dimensionless nanofluid velocity, $\hat{k} = (0,0,1)$ is the unit vector in the z – direction, $P_r = \frac{\mu}{\rho\kappa_T}$ is the Prandtl number, $D_a = \frac{k_1\bar{\mu}}{\mu d^2}$ is the Darcy number, $\tau_n = \frac{\kappa_T}{D_B}$ is the Nanofluid Lewis number, $\tau_s = \frac{\kappa_T}{D_S}$ is the solute Lewis number, $R_a = \frac{\rho g\alpha_T k_1 d(T_0-T_1)}{\mu\kappa_T}$ is the thermal Darcy-Rayleigh number, $R_s = \frac{\rho g\alpha_C k_1 d(C_0-C_1)}{\mu D_S}$ is the solute Rayleigh number, $R_n = \frac{(\rho_P-\rho)(\varphi_1-\varphi_0)gk_1d}{\mu\kappa_T}$ is the Nanoparticle concentration Rayleigh number, $R_m = \frac{[\rho_P\varphi_0+\rho(1-\varphi_0)]gk_1d}{\mu\kappa_T}$ is the basic-density Rayleigh number, $R_i = \frac{G_0d^2}{K_m}$ is the internal Rayleigh number, $T_a = \frac{4\Omega^2d^4\rho^2}{\epsilon^2\mu^2}$ is the Taylor number, $N_A = \frac{D_T(T_0-T_1)}{D_BT_1(\varphi_1-\varphi_0)}$ is the Diffusivity ratio, $N_B = \frac{\epsilon(\rho c)_P}{(\rho c)_f}(\varphi_1-\varphi_0)$ is the particle density increment, $N_{TC} = \frac{D_{TC}(C_0-C_1)}{\kappa_T(T_0-T_1)}$ is the Dufour parameter, $N_{CT} = \frac{D_{CT}(T_0-T_1)}{\kappa_T(C_0-C_1)}$ is the Soret parameter.

The boundary conditions (6)-(7) in non-dimensional form become

$w = 0, T = 1, C = 1, \varphi = 0$ at $z = 0,$ (14)

$w = 0, T = 0, C = 0, \varphi = 1$ at $z = 1.$ (15)

The basic state of nanofluid is assumed to be static state and is given by

$$\boldsymbol{q} = \boldsymbol{q}_b = (0,0,0),\ p = p_b(z),\ T = T_b(z),\ C = C_b(z),\ \varphi = \varphi_b(z). \tag{16}$$

Using the basic state in Eqs. (9) – (13), we get the following basic state solutions as given by

$$T_b = \frac{\sin\sqrt{R_i}(1-z)}{\sin\sqrt{R_i}},\ C_b = 1 - z + N_{CT}\tau_s\left(1 - z - \frac{\sin\sqrt{R_i}(1-z)}{\sin\sqrt{R_i}}\right),\ \varphi_b = z + N_A\left(1 - z - \frac{\sin\sqrt{R_i}(1-z)}{\sin\sqrt{R_i}}\right). \tag{17}$$

Now we analyze the stability of basic state by introducing the following perturbations:

$$\boldsymbol{q} = \boldsymbol{q}_b + \boldsymbol{q}',\ p = p_b(z) + p',\ T = T_b(z) + \theta',\ C = C_b(z) + \phi',\ \varphi = \varphi_b(z) + \varphi'. \tag{18}$$

where $\boldsymbol{q}' = (u', v', w')$, p', θ', ϕ' and $\varphi'$are perturbations in nanofluid velocity, pressure, temperature, concentration and nanoparticle volume fraction respectively and are assumed to be small.

Using Eqs. (18) into Eqs. (9)-(13) and using the basic state solutions, we obtain the following linearized perturbation equations

$$\frac{\partial u'}{\partial x} + \frac{\partial v'}{\partial y} + \frac{\partial w'}{\partial z} = 0, \tag{19}$$

$$\frac{D_a}{P_r}\frac{\partial u'}{\partial t} = -\frac{\partial p'}{\partial x} + D_a\nabla^2 u' - u' + \sqrt{T_a}\, v', \tag{20}$$

$$\frac{D_a}{P_r}\frac{\partial v'}{\partial t} = -\frac{\partial p'}{\partial y} + D_a\nabla^2 v' - v' - \sqrt{T_a} u', \tag{21}$$

$$\frac{D_a}{P_r}\frac{\partial w'}{\partial t} = -\frac{\partial p'}{\partial z} + D_a\nabla^2 w' - w' + R_a\theta' + \frac{R_s}{\tau_s}\phi' - R_n\varphi', \tag{22}$$

$$\frac{\partial \theta'}{\partial t} + \frac{\partial T_b}{\partial z}w' = \nabla^2\theta' + \frac{N_B}{\tau_n}\left[\frac{\partial \theta'}{\partial z} - \frac{\partial \varphi'}{\partial z}\right] - 2\frac{N_A N_B}{\tau_n}\frac{\partial \theta'}{\partial z} + N_{TC}\nabla^2\phi' + R_i\,\theta', \tag{23}$$

$$\frac{1}{\gamma}\frac{\partial \phi'}{\partial t} - \frac{1}{\epsilon}w' = \frac{1}{\tau_s}\nabla^2\phi' + N_{CT}\nabla^2\theta', \tag{24}$$

$$\frac{1}{\gamma}\frac{\partial \varphi'}{\partial t} + \frac{1}{\epsilon}w' = \frac{1}{\tau_n}\nabla^2\varphi' + \frac{\mathrm{N_A}}{\tau_\mathrm{n}}\nabla^2\theta'. \tag{25}$$

The normal mode expansion of the dependent variables $u', v', w', p', \theta', \phi'$ and φ' is assumed in the form

$$F'(x, y, z, t) = F''(z)\exp[i(k_x x + k_y y) + \sigma t], \tag{26}$$

where k_x and k_y are the wave numbers along x and y directions respectively, $a = \sqrt{k_x^2 + k_y^2}$ is the resultant wave number and σ is a complex constant in general. For functions with this dependence on *x*, *y* and *t*, we have

$$\frac{\partial}{\partial t} = \sigma,\ \frac{\partial^2}{\partial x^2} + \frac{\partial^2}{\partial y^2} = -a^2 \text{ and } \nabla^2 = \frac{d^2}{dz^2} - a^2 \tag{27}$$

Eqs. (19)-(25), then become

$$ik_x u'' + ik_y v'' + \frac{dw''}{dz} = 0, \tag{28}$$

$$\frac{D_a}{P_r}\sigma u'' = -ik_x p'' + D_a\left(\frac{d^2}{dz^2} - a^2\right)u'' - u'' + \sqrt{T_a}v'', \tag{29}$$

$$\frac{D_a}{P_r}\sigma v'' = -ik_y p'' + D_a\left(\frac{d^2}{dz^2} - a^2\right)v'' - v'' - \sqrt{T_a}u'', \tag{30}$$

$$\frac{D_a}{P_r}\sigma w'' = -\frac{dp''}{dz} + D_a\left(\frac{d^2}{dz^2} - a^2\right)w'' - w'' + R_a\theta'' + \frac{R_s}{\tau_s}\phi'' - R_n\varphi'', \tag{31}$$

$$\sigma\theta'' + \frac{dT_b}{dz}w'' = \left(\frac{d^2}{dz^2} - a^2\right)\theta'' + \frac{N_B}{\tau_n}\left[\frac{d\theta''}{dz} - \frac{d\varphi''}{dz}\right] - 2\frac{N_A N_B}{\tau_n}\frac{d\theta''}{dz} + N_{TC}\left(\frac{d^2}{dz^2} - a^2\right)\phi'' + R_i\theta'', \tag{32}$$

$$\frac{\sigma}{\gamma}\phi'' - \frac{1}{\epsilon}w'' = \frac{1}{\tau_s}\left(\frac{d^2}{dz^2} - a^2\right)\phi'' + N_{CT}\left(\frac{d^2}{dz^2} - a^2\right)\theta'', \tag{33}$$

$$\frac{\sigma}{\gamma}\varphi'' + \frac{1}{\epsilon}w'' = \frac{1}{\tau_n}\left(\frac{d^2}{dz^2} - a^2\right)\varphi'' + \frac{\mathrm{N_A}}{\mathrm{\tau_n}}\left(\frac{d^2}{dz^2} - a^2\right)\theta''. \tag{34}$$

Eliminating u'' and v'' from Eqs. (29) and (30) by multiplying Eq. (29) by ik_x and (30) by ik_y respectively, adding the resulting equations and using Eq. (28), and then eliminating p'' between this resulting equation and Eq. (31), we obtain

$$D_a\left(\frac{d^2}{dz^2} - a^2\right)^2 w'' - \left(1 + \frac{D_a\sigma}{P_r}\right)\left(\frac{d^2}{dz^2} - a^2\right)w'' - R_a a^2\theta'' - \frac{R_s}{\tau_s}a^2\phi'' + R_n a^2\varphi'' - \sqrt{T_a}\frac{d\zeta''}{dz} = 0, \tag{35}$$

Where $\zeta'' = i\left(k_x v'' - k_y u''\right)$, (36)

is the z – component of vorticity.

In order to obtain an equation governing ζ'', multiplying equations (29) and (30) by ik_y and ik_x respectively, subtracting the former resulting equation from the latter resulting equation and then making use of equations (28) and (36), we obtain

$$D_a\left(\frac{d^2}{dz^2} - a^2\right)\zeta'' - \left(1 + \frac{D_a\sigma}{P_r}\right)\zeta'' + \sqrt{T_a}\frac{dw''}{dz} = 0. \tag{37}$$

Now we can transform Eqs. (32) – (37) into the following non-dimensional form in terms of w, θ, ϕ, φ, and ζ (omitting the primes for simplicity in writing)

$$D_a(D^2 - a^2)\left(D^2 - a^2 - \frac{\sigma}{P_r}\right)w - (D^2 - a^2)w - R_a a^2\theta - \frac{R_s}{\tau_s}a^2\phi + R_n a^2\varphi - \sqrt{T_a}D\zeta = 0, \tag{38}$$

$$(D^2 - a^2 - \sigma + R_i)\,\theta + \left(\frac{N_B}{\tau_n}D - 2\frac{N_A N_B}{\tau_n}D\right)\theta - \frac{N_B}{\tau_n}D\varphi + N_{TC}(D^2 - a^2)\phi - f(z)w = 0, \tag{39}$$

$$\left[\frac{\epsilon}{\tau_s}(D^2 - a^2) - \eta\sigma\right]\phi + \epsilon N_{CT}(D^2 - a^2)\theta + w = 0, \tag{40}$$

$$\left[\frac{\epsilon}{\tau_n}(D^2-a^2)-\eta\sigma\right]\varphi+\frac{\epsilon N_A}{\tau_n}(D^2-a^2)\theta-w=0, \tag{41}$$

$$D_a\left(D^2-a^2-\frac{\sigma}{P_r}-{D_a}^{-1}\right)\zeta+\sqrt{T_a}Dw=0, \tag{42}$$

with boundary conditions

$$w=0=\theta=\phi=\varphi=D^2w=D\zeta \text{ at } z=0 \text{ and } z=1, \tag{43}$$

(both the boundaries are free)

where z is the real independent variable such that $0\le z\le 1$, $D=\frac{d}{dz}$ is differentiation with respect to z, $f(z)=\frac{dT_b}{dz}=-\sqrt{R_i}\frac{cos\sqrt{R_i}(1-z)}{sin\sqrt{R_i}}$, $\eta(=\frac{\epsilon}{\gamma})>0$ is the normalized porosity, a^2 is square of the wave number, $P_r>0$ is the Prandtl number, σ is the complex growth rate, $D_a>0$ is the Darcy number, $T_a>0$ is the Taylor number, $\tau_s>0$ is the solute Lewis number, $\tau_n>0$ is the nanofluid Lewis number, $N_A>0$ is a constant diffusivity ratio, $N_B>0$ is a constant particle density increment, $N_{TC}>0$ is a constant Dufour parameter, $N_{CT}>0$ is a constant Soret parameter, $R_a>0$ is the thermal Darcy-Rayleigh number, $R_s>0$ is the solute Rayleigh number, $R_n>0$ is the nanoparticle concentration Rayleigh number, $R_i>0$ is the internal Rayleigh number, w is the vertical velocity, θ is the temperature, ϕ is the concentration, φ is the volume fraction of nanoparticles and ζ is the z-component of the vorticity.

It may further be noted that Eqs. (38) - (43) describe an eigenvalue problem for σ and govern Double-Diffusive Nanofluid convection in a porous medium heated and salted from below with the presence of internal heat source and rotation for the case of free boundaries.

3. Mathematical analysis

Operating Eq. (38) with the operator $D_a\left(D^2-a^2-\frac{\sigma}{P_r}-{D_a}^{-1}\right)$ throughout we obtain the following equation

$$D_a^2(D^2-a^2)\left(D^2-a^2-\frac{\sigma}{P_r}-{D_a}^{-1}\right)\left(D^2-a^2-\frac{\sigma}{P_r}\right)w-D_a(D^2-a^2)\left(D^2-a^2-\frac{\sigma}{P_r}-{D_a}^{-1}\right)w-R_aa^2D_a\left(D^2-a^2-\frac{\sigma}{P_r}-{D_a}^{-1}\right)\theta-\frac{R_s}{\tau_s}a^2D_a\left(D^2-a^2-\frac{\sigma}{P_r}-{D_a}^{-1}\right)\phi+R_na^2D_a\left(D^2-a^2-\frac{\sigma}{P_r}-{D_a}^{-1}\right)\varphi+T_aD^2w=0, \tag{44}$$

To satisfy boundary conditions (43), we assume the solution for w, θ, ϕ, φ, and ζ in the form

$$w=W_0 sin\pi z,\ \theta=\Theta_0 sin\pi z,\ \phi=\Phi_0 sin\pi z,\ \varphi=Ꝏ_0 sin\pi z, \tag{45}$$

where W_0, Θ_0, Φ_0 and $Ꝏ_0$ are constants. Substituting Eq. (45) into Eq. (44) and Eqs. (39)–(41), multiplying the resulting equations by $sin\pi z$, and integrating each equation from $z = 0$ to $z = 1$ and performing some integration by parts, we obtain the following matrix equation

$$\begin{bmatrix} A_1^2 J + T_a\pi^2 & -R_a a^2 A_1 & -(R_s/\tau_s)a^2 A_1 & R_n a^2 A_1 \\ 2F & A_2 & N_{TC}J & 0 \\ -1 & \epsilon N_{CT}J & A_3 & 0 \\ 1 & (\epsilon N_A/\tau_n)J & 0 & A_4 \end{bmatrix} \begin{bmatrix} W_0 \\ \Theta_0 \\ \Phi_0 \\ \Omega_0 \end{bmatrix} = \begin{bmatrix} 0 \\ 0 \\ 0 \\ 0 \end{bmatrix}, \quad (46)$$

where $J = \pi^2 + a^2$ is the total wave number, $F = \int_0^1 f(z) sin^2 \pi z dz = \frac{-2\pi^2}{4\pi^2 - R_i}$,

$$A_1 = D_a(J + \frac{\sigma}{P_r} + D_a{}^{-1}), \quad (47)$$

$$A_2 = (J + \sigma - R_i), \quad (48)$$

$$A_3 = (\frac{\epsilon}{\tau_s}J + \eta\sigma), \quad (49)$$

and $A_4 = (\frac{\epsilon}{\tau_n}J + \eta\sigma).$ (50)

The above system of homogeneous equations admits a non-trivial solution only if its determinant is equal to zero which on solving yields the characteristic equation of the system. This characteristic equation gives the following expression for the thermal Darcy-Rayleigh number R_a

$$R_a = (-2FA_3 - N_{TC}J)^{-1}\left[\left\{\frac{J}{a^2}A_1 + \frac{T_a\pi^2}{a^2 A_1} - \frac{R_n}{A_4}\right\}(A_2A_3 - \epsilon N_{TC}N_{CT}J^2) - \frac{R_s}{\tau_s}(2F\epsilon N_{CT}J + A_2)\right] - \frac{R_n N_A \frac{\epsilon}{\tau_n} J}{A_4}. \quad (51)$$

The growth rate σ is a complex constant in general such that $\sigma = \tau + i\omega$, where τ and ω are respectively the real and imaginary parts of σ. The system is always stable if $\text{Re}(\sigma) < 0$ while it will become unstable if $\text{Re}(\sigma) > 0$. For neutral stability we have $\text{Re}(\sigma) = 0$.

3.1 Stationary convection

For the validity of the "principle of exchange of stabilities" (stationary convection), we have $\sigma = 0$ (i.e. $\tau = \omega = 0$) at the marginal stability. Then Eq. (51) reduces to

$$R_a = (-2F - \frac{\tau_s N_{TC}}{\epsilon})^{-1}\left[\left\{\frac{D_a J^3}{a^2} + \frac{J^2}{a^2} + \frac{J\pi^2 T_a}{a^2(1+D_aJ)} - \frac{\tau_n}{\epsilon}R_n\right\}\left(1 - \frac{R_i}{J} - N_{TC}N_{CT}\tau_s\right) - R_s(\frac{1}{\epsilon} - \frac{R_i}{\epsilon J} + 2FN_{CT})\right] - R_n N_A. \quad (52)$$

Special case:

In the absence of internal heat source i.e. $G_0 = 0$, we have $R_i = 0$ and $F = -1/2$, we obtain

$$R_a = (1 - \frac{\tau_s N_{TC}}{\epsilon})^{-1}\left[\left\{\frac{D_a J^3}{a^2} + \frac{J^2}{a^2} + \frac{J\pi^2 T_a}{a^2(1+D_aJ)} - \frac{\tau_n}{\epsilon}R_n\right\}(1 - N_{TC}N_{CT}\tau_s) - R_s(\frac{1}{\epsilon} - N_{CT})\right] - R_n N_A, \quad (53)$$

an expression as obtained by Sharma and Gupta [34]. Again if $\tau_s = 0$, $R_s = 0$ and $T_a = 0$, we obtain

$$R_a = \frac{D_a(\pi^2+a^2)^3}{a^2} + \frac{(\pi^2+a^2)^2}{a^2} - \left(\frac{\tau_n}{\epsilon} + N_A\right) R_n. \tag{54}$$

This is the same expression for thermal Rayleigh-Darcy number as obtained by Kuznetsov and Nield [24].

For the case when $D_a = 0$, the minimum is attained with $a = \pi$ and the minimum value is

$$R_a = 4\pi^2 - \left(\frac{\tau_n}{\epsilon} + N_A\right) R_n.$$

On the other hand, in the case where D_a is large compared with unity, the minimum being attained at $a = \frac{\pi}{\sqrt{2}}$, and the minimum value is

$$R_a = \frac{27\pi^4}{4} D_a - \left(\frac{\tau_n}{\epsilon} + N_A\right) R_n.$$

In the absence of nanoparticles, one recovers the well-known results that the critical Rayleigh-Darcy number (Lapwood [25]) is equal to $4\pi^2$ when $D_a = 0$, and that the critical value of the fluid Rayleigh-number Chandrasekhar [11] is $\frac{27\pi^4}{4} = 657.5$ in the case where D_a tends to infinity.

3.2 Oscillatory convection

For oscillatory convection, we put $\sigma = i\omega$, where ω =Im(σ) (Re(σ) $= \tau = 0$) in the eigenvalue equation (51). Assuming Lewis number and Prandtl number approaching to infinity with Dufour and Soret parameters negligible and heat capacity ratio as unity, the real and imaginary parts of equation (51) can be written as

$$\frac{-J}{2Fa^2}\left(1 - \frac{\omega^2}{J^2} - \frac{R_i}{J}\right)\left(J + D_a J^2 + \frac{\pi^2 T_a}{(1+D_a J)}\right) = R_a - \frac{1}{2F}\left(2 - \frac{R_i}{J}\right)\frac{R_n}{\epsilon} - \frac{1}{2F}\left(1 - \frac{R_i}{J}\right)\frac{R_s}{\epsilon} \tag{55}$$

and

$$\frac{-(2J-R_i)}{2Fa^2}\left(J + D_a J^2 + \frac{\pi^2 T_a}{(1+D_a J)}\right) = R_a + \frac{J^2}{2F}\left(1 - \frac{\omega^2}{J^2} - \frac{R_i}{J}\right)\frac{R_n}{\epsilon\omega^2} - \frac{1}{2F}\frac{R_s}{\epsilon}. \tag{56}$$

Solving Eqns. (57) and (58), we obtain

$$a_1(\omega^2)^2 + a_2\omega^2 + a_3 = 0, \tag{57}$$

where $a_1 = N$, (58)

$$a_2 = J^2 N + (J - R_i)R_n - R_i R_s, \tag{59}$$

$$a_3 = J^2(J - R_i)R_n \tag{60}$$

and

$$N = \frac{\epsilon}{a^2}\left(J + D_a J^2 + \frac{\pi^2 T_a}{(1+D_a J)}\right). \tag{61}$$

Special case:

In the absence of internal heat source i.e. $G_0 = 0$, we have $R_i = 0$ and $F = -1/2$, Eqs. (57) to (61) yields

$$\frac{J}{a^2}\left(1 - \frac{\omega^2}{J^2}\right)\left(J + D_a J^2 + \frac{\pi^2 T_a}{(1+D_a J)}\right) = R_a + \frac{2R_n}{\epsilon} + \frac{R_s}{\epsilon}, \tag{62}$$

$$\frac{2J}{a^2}\left(J + D_a J^2 + \frac{\pi^2 T_a}{(1+D_a J)}\right) = R_a - \frac{J^2 R_n}{\epsilon\omega^2} + \frac{R_n}{\epsilon} + \frac{R_s}{\epsilon} \tag{63}$$

and

$$\omega^2 = -a^2 R_n \left(\epsilon\left(1 + D_a J + \frac{\pi^2 T_a}{(1+D_a J)J}\right)\right)^{-1}, \tag{64}$$

which are the same expressions as derived by Sharma and Gupta [34].

It is worth to point out from Eq. (57) that if $J > R_i$ $J > R_i(R_n + R_s)$then all coefficients are positive. Thus, Eq. (57) does not have any positive value for ω^2.

Thus, no oscillatory instability is possible if $J > R_i$ and $J > R_i(R_n + R_s)$.

4. Results and discussion

In the present work, the effect of internal heat source and rotation on the onset of double-diffusive convection in a nanofluid layer saturating a sparsely distributed porous medium heated and soluted from below, has been investigated using Darcy-Brinkman model. The problem has been studied analytically and numerically by using the software MATHEMATICA. The marginal stability curves for stationary mode are depicted through various figures for fixed values of different parameters. The variation of thermal Darcy-Rayleigh number R_a with wave number a is plotted in Figs. (2)-(11). The values of various parameters are assumed as $\tau_s = 2, \tau_n = 5000, T_a = 500, R_s = 200, N_{TC} = 0.001, N_{CT} = 1, \epsilon = 0.6, D_a = 0.7$ (Sharma and Gupta [34]).

In the present study, the results depicted in Figs. (2)-(10) are discussed for alumina nanoparticle ($N_A = 5$, $R_n = 0.06$). The impact of the internal heat source on the onset of stationary convection in a nanofluid layer is depicted in Fig. 2 which demonstrates that an increase in internal Rayleigh number R_i results in a spontaneous decrease in the Rayleigh number. This is due to the fact that the system becomes more unstable due to the enhanced energy supply, leading to greater disturbances within the nanofluid layer. Further, Fig. 3 illustrates that the solute Rayleigh number R_s has a destabilizing effect on the system in the presence of internal heat source which is contrary to the case of classical thermohaline convection problem wherein the effect is stabilizing.

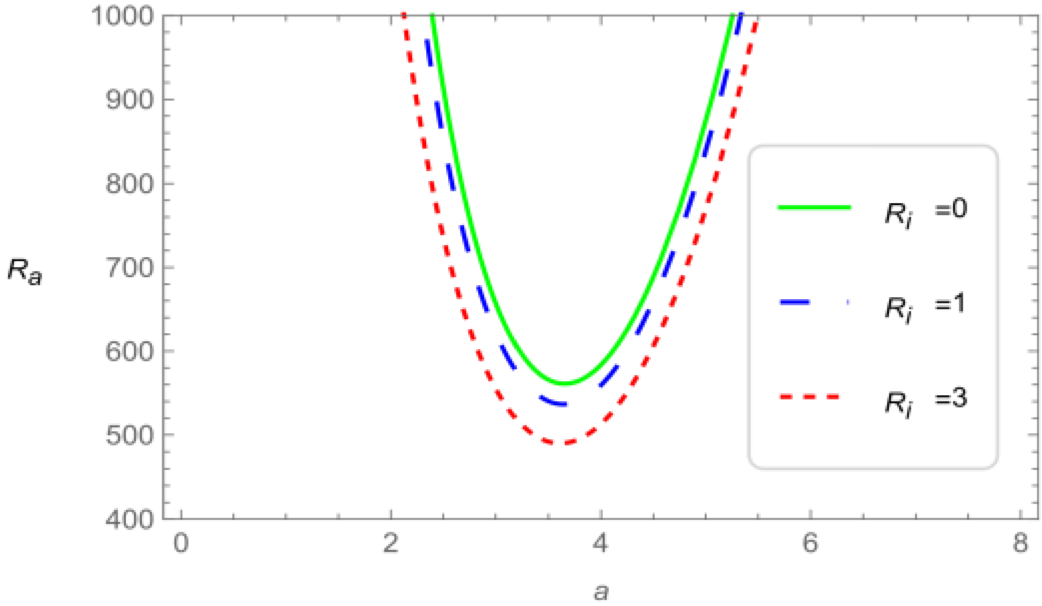

Fig. 2: R_a vs a for different values of R_i with $D_a = 0.7$, $T_a = 500, N_A = 5, N_{CT} = 1$, $N_{TC} = 0.001$, $R_s = 200$, $R_n = 0.06, \tau_n = 5000$, $\tau_s = 2$ and $\varepsilon = 0.6$.

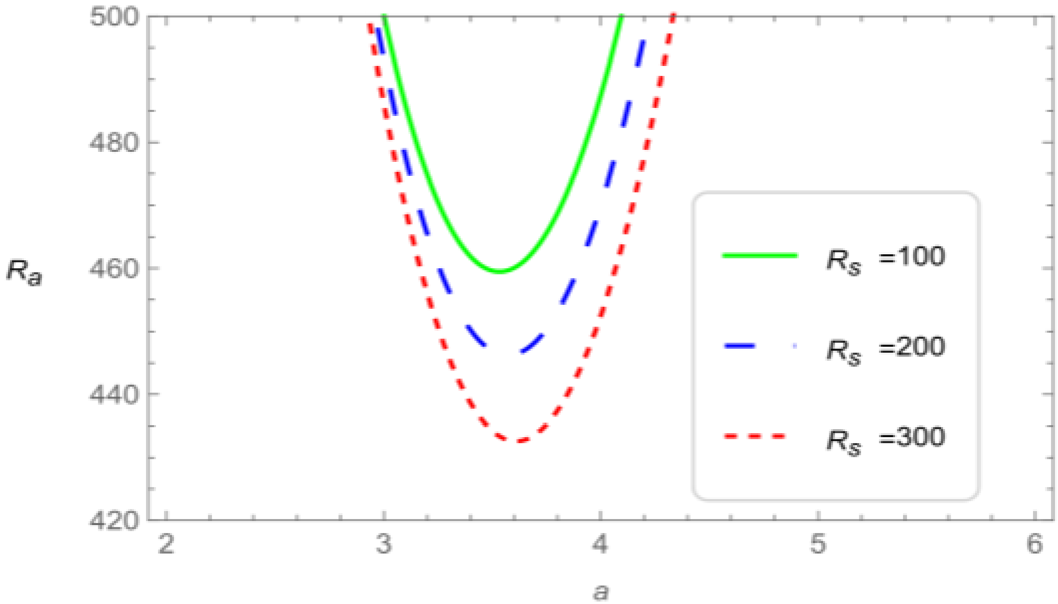

Fig. 3: R_a vs a for different values of R_s with $D_a = 0.7, T_a = 500, N_A = 5, N_{CT} = 1, N_{TC} = 0.001, R_s = 200$, $R_n = 0.06, R_i = 1, \tau_n = 5000$, $\tau_s = 2$ and $\varepsilon = 0.6$.

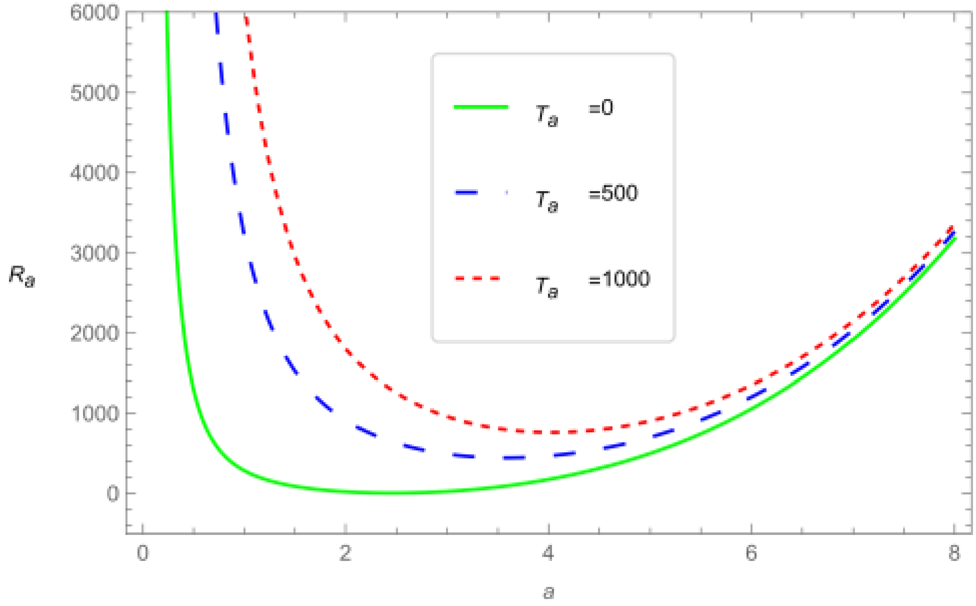

Fig. 4: R_a vs a for different values of T_a with $D_a = 0.7, N_A = 5, N_{CT} = 1, N_{TC} = 0.001, R_s = 200,\ R_n = 0.06, R_i = 1, \tau_n = 5000,\ \tau_s = 2$ and $\varepsilon = 0.6$.

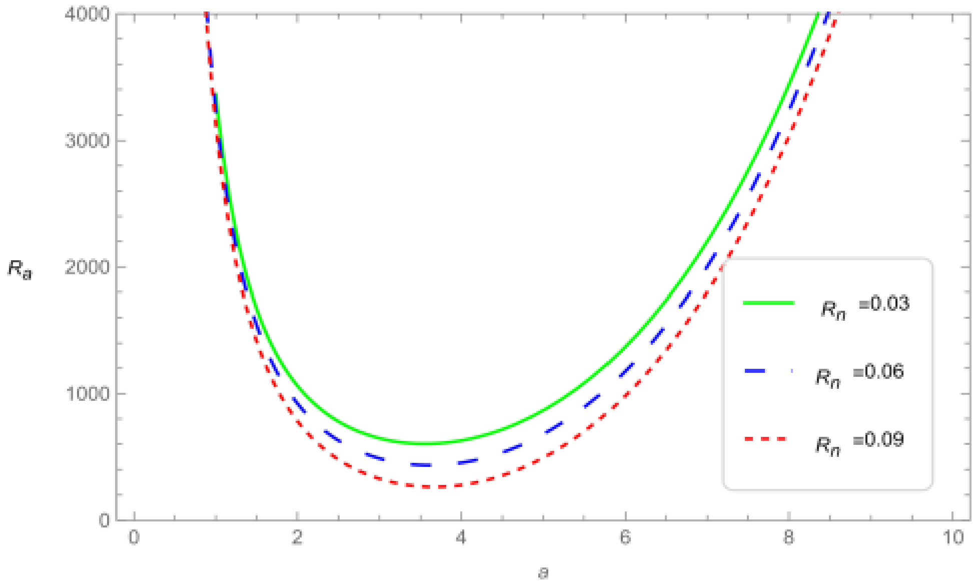

Fig. 5: R_a vs a for different values of R_n with $D_a = 0.7, T_a = 500, N_A = 5, N_{CT} = 1,\ N_{TC} = 0.001\ ,\ R_s = 200, R_i = 1, \tau_n = 5000,\ \tau_s = 2$ and $\varepsilon = 0.6$.

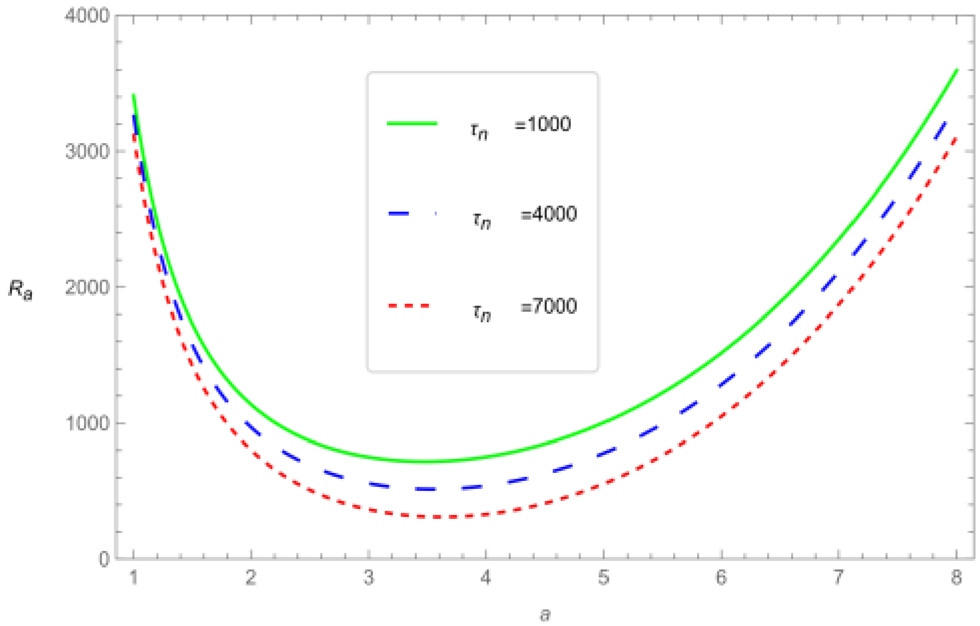

Fig. 6: $\boldsymbol{R_a}$ vs $\boldsymbol{a}$ for different values of $\boldsymbol{\tau_n}$ with $\boldsymbol{D_a = 0.7, T_a = 500, N_A = 5, N_{CT} = 1, N_{TC} = 0.001, R_s = 200, R_n = 0.06, R_i = 1, \tau_s = 2}$ and $\boldsymbol{\varepsilon = 0.6}$.

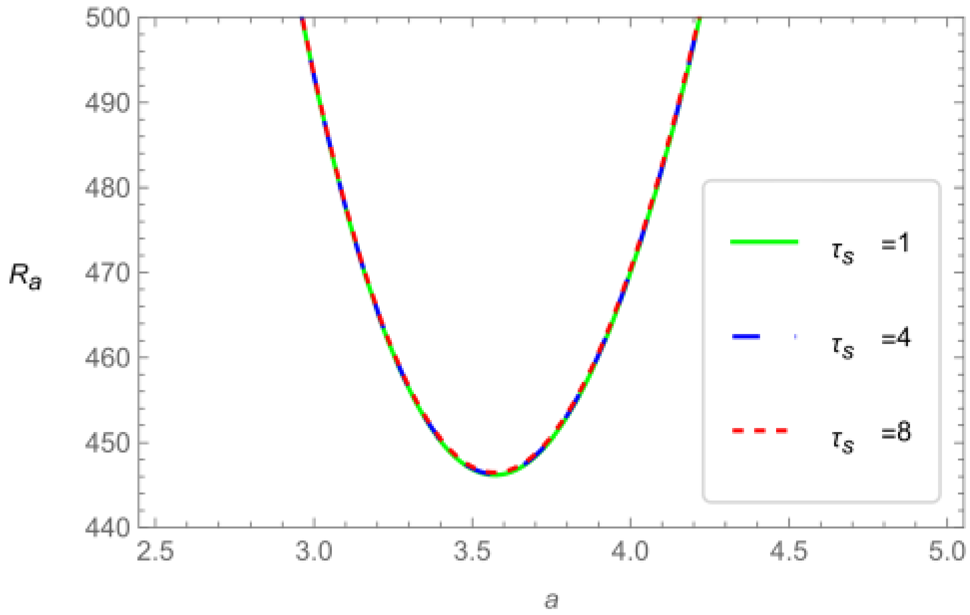

Fig. 7: $\boldsymbol{R_a}$ vs $\boldsymbol{a}$ for different values of $\boldsymbol{\tau_s}$ with $\boldsymbol{D_a = 0.7, T_a = 500, N_A = 5, N_{CT} = 1, N_{TC} = 0.001, R_s = 200, R_n = 0.06, R_i = 1, \tau_n = 5000}$ and $\boldsymbol{\varepsilon = 0.6}$.

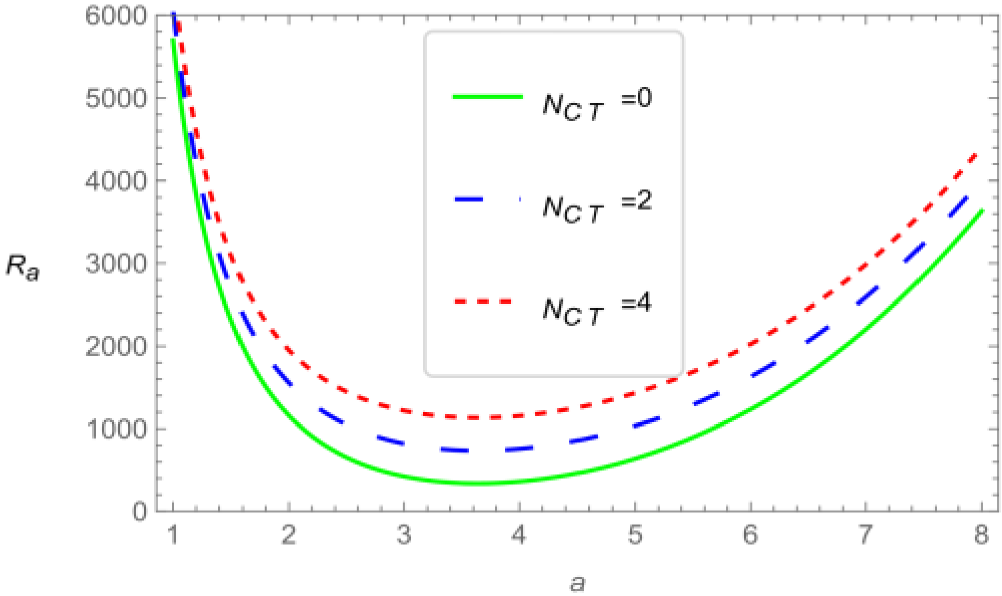

Fig. 8: $\boldsymbol{R_a}$ vs $\boldsymbol{a}$ for different values of $\boldsymbol{N_{CT}}$ with $\boldsymbol{D_a = 0.7, T_a = 500, N_A = 5, N_{TC} = 0.001, R_s = 200, R_n = 0.06, R_i = 1, \tau_n = 5000, \tau_s = 2}$ and $\boldsymbol{\varepsilon = 0.6}$.

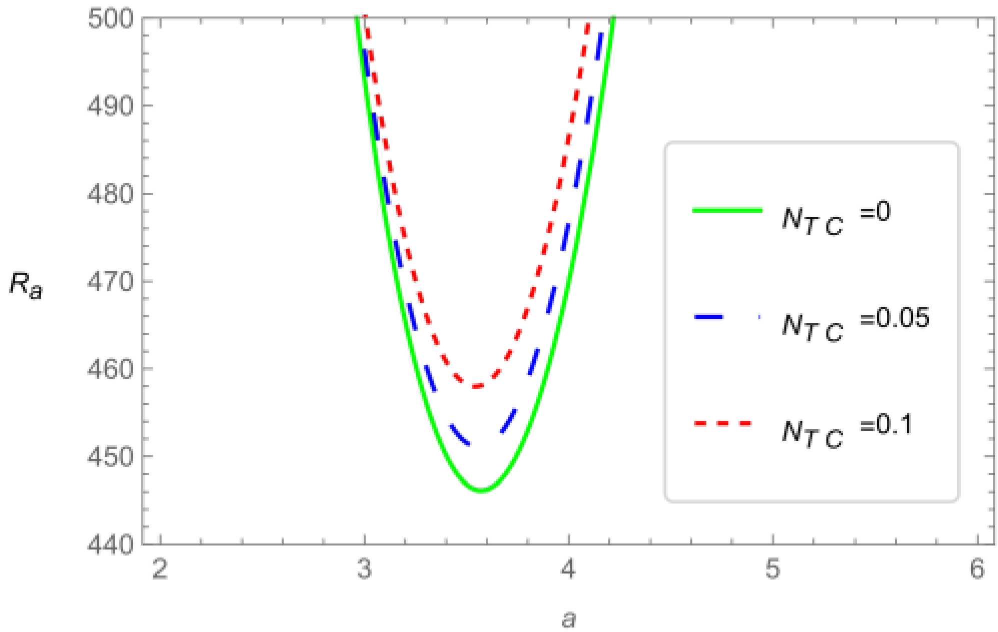

Fig. 9: $\boldsymbol{R_a}$ vs $\boldsymbol{a}$ for different values of $\boldsymbol{N_{TC}}$ with $\boldsymbol{D_a = 0.7, T_a = 500, N_A = 5, N_{CT} = 1, R_s = 200, R_n = 0.06, R_i = 1, \tau_n = 5000, \tau_s = 2, \varepsilon = 0.6}$.

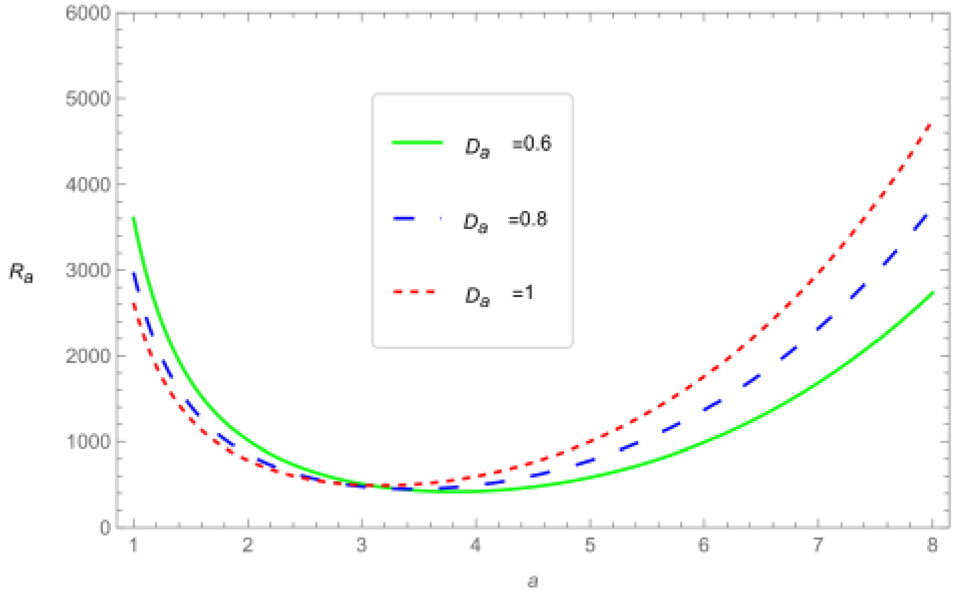

Fig. 10: $\boldsymbol{R_a}$ vs $\boldsymbol{a}$ for different values of $\boldsymbol{D_a}$ with $\boldsymbol{T_a = 500, N_A = 5, N_{CT} = 1, N_{TC} = 0.001, R_s = 200, R_n = 0.06, R_i = 1, \tau_n = 5000, \tau_s = 2}$ and $\boldsymbol{\varepsilon = 0.6}$.

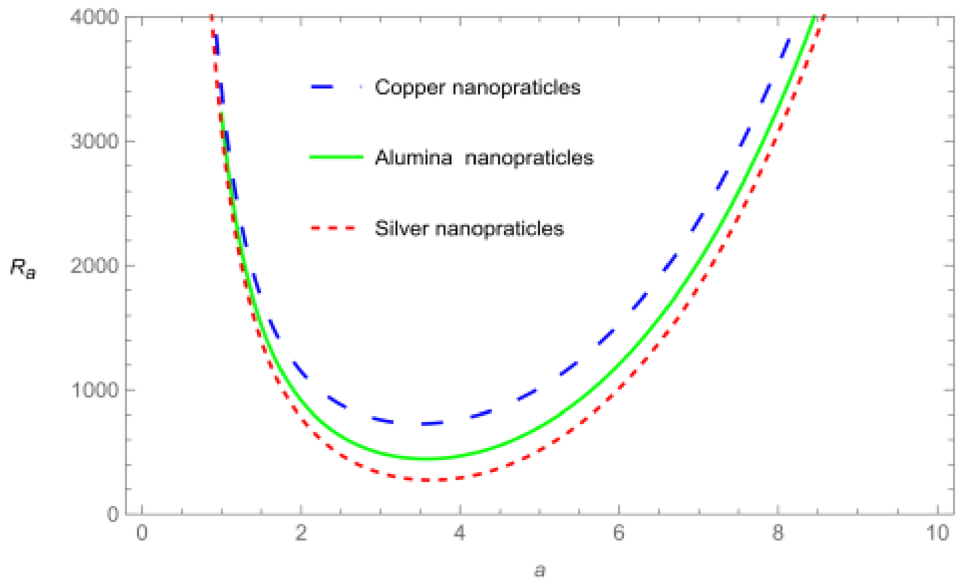

Fig.11: Effect of different nanoparticles on Rayleigh number $\boldsymbol{R_a}$. Alumina nanoparticles ($\boldsymbol{N_A = 0.5, R_n = 0.06}$), copper nanoparticles ($\boldsymbol{N_A = 5, R_n = 0.01}$) and silver nanoparticles ($\boldsymbol{N_A = 5, R_n = 0.09}$)where $\boldsymbol{D_a = 0.7, T_a = 500, N_{CT} = 1, N_{TC} = 0.001, R_s = 200, R_i = 1, \tau_n = 5000, \tau_s = 2}$ and $\boldsymbol{\varepsilon = 0.6}$.

The effect of Taylor number T_a on the thermal Darcy-Rayleigh number R_a against the wave number a is shown in Fig. 4. It is clear from this figure that rotation has a stabilizing influence on the stability of the nanofluid layer. This indicates that the Coriolis force resulting from rotation inhibits the onset of stationary convection in the nanofluid layer. Since the nanoparticle concentration Rayleigh number R_n is directly proportional to the nanoparticle volume fraction φ. Thus, an increase in the nanoparticle concentration Rayleigh number will increase the nanoparticle volume fraction as a result of a combination of Brownian motion and thermophoresis diffusion within the nanofluid layer, thus destabilizing the system, as seen clearly in Fig. 5. The effects of nanofluid Lewis number and solute Lewis number on thermal Darcy-Rayleigh number are shown in Figs. (6) and (7) respectively. The destabilizing influence of the nanofluid Lewis number can be seen in Fig. (6). However, the solute Lewis number's stabilizing influence on the fluid layer's stability is so small that it is not reflected in Fig. (7). The impacts of two important types of interdiffusion, that is Soret and Dufour parameters (arising due to the combination of temperature and concentration gradients in a nanofluid system) are depicted in Figs. 8 and 9, respectively. In Fig. 8, the values of Rayleigh number increase as the Soret parameter increases and thus stabilizes the system. The influence of the Dufour parameter is also stabilizing on the system as can be seen in Fig. 9. Fig.10 shows that Darcy number D_a has dual effect. It is found that for small values of wave number, the Darcy number D_a has a destabilizing effect on the system while for large values of wave number the effect of D_a is reversed. The Effects of different nanoparticles viz. alumina nanoparticles ($N_A = 0.5$, $R_n = 0.06$), copper nanoparticles ($N_A = 5$, $R_n = 0.01$) and silver nanoparticles ($N_A = 5$, $R_n = 0.09$) on Rayleigh number with internal Rayleigh number $R_i = 5$ are shown in Fig.11. Among the nanofluids analyzed, copper-water is the most stable, followed by alumina-water, with silver-water being the least stable.

5. Conclusion

The study examines double-diffusive convection in a horizontal layer of nanofluid within a sparsely distributed porous medium, considering the effects of rotation and an internal heat source under free boundary conditions. The findings reveal that the internal heat source destabilizes the system. The Darcy number exhibits a dual effect: it destabilizes the system for small wave numbers but stabilizes it for large wave numbers. Parameters such as rotation, Dufour, and Soret have stabilizing influence, whereas the nanoparticle concentration Rayleigh number has a destabilizing effect on the system. Among the nanofluids analyzed, copper-water is the most stable, followed by alumina-water, with silver-water being the least stable.

Acknowledgement: The authors are thankful to the referee for valuable comments and suggestions.

References

[1] Agarwal, S., Sacheti, N.C., Chandran, P., Bhadauria, B.S. and Singh, A.K. (2012). Non-linear convective transport in a binary nanofluid saturated porous layer, Transp. Porous Media., **93**, 29-49.

[2] Akhila, P. A., Mallikarjun, B. P., Kiran, P. and Chamkha, A. J. (2024). Study of double-diffusive gravity modulated biothermal convection in porous media under internal heating effect, Eur. Phys. J. Plus., **139**, 1-19.

[3] Ali, S. A., Rudziva, M., Sibanda, P., Noreldin, O. A., Goqo, S. P. and Mthethwa, H. S. (2022). A numerical study of double-diffusive convection in the anisotropic porous layer under rotational modulation with internal heat generation, Int. Commun. Heat Mass Transf., **137**, 106266.

[4] Awasthi, M.K., Kumar, V. and Patel, R.K. (2018). Onset of triply diffusive convection in a Maxwell fluid saturated porous layer with internal heat source, Ain Shams Eng. J, **9**, 1591-1600.

[5] Bhadauria, B.S. and Srivastava, A. (2022). Combined effect of internal heating and through-flow in a nanofluid saturated porous medium under local thermal nonequilibrium, J. Porous Media, **25**, 75-95.

[6] Bhadauria, B.S. and Agarwal, S. (2011). Natural convection in a nanofluid saturated rotating porous layer: a nonlinear study, Int. J. Therm. Sci, **87**, 585-602.

[7] Bhadauria, B.S., Kumar, A., Kumar, J., Sacheti, N.C. and Chandran, P. (2011). Natural convection in a rotating anisotropic porous layer with internal heat generation., Transp. Porous Media, **90**, 687-705.

[8] Bhattacharyya, S.P. and Jena, S.K. (1984). Thermal instability of a horizontal layer of micropolar fluid with heat source, Proc. Math. Sci, **93**, 13-26.

[9] Buongiorno, J. (2005). Convective Transport in Nanofluids, J. Heat Transf, **128**, 240-250.

[10] Chamkha, A.J, Mansour, M.A., Rashad, A.M., Kargarsharifabad, H. and Armaghani, T. (2020). Magnetohydrodynamic mixed convection and entropy analysis of nanofluid in gamma-shaped porous cavity, J. Thermophys. Heat Transf, **34,** 836-847.

[11] Chandrasekhar, S. (1981). Hydrodynamic and Hydromagnetic Stability, Dover publication, Inc., New York.

[12] Char, M.I. and Chiang, K.T. (1994). Stability analysis of Benard-Marangoni convection in fluids with internal heat generation, J. Phys. D Appl. Phys, **27,** 748.

[13] Choi, S. (1995). Enhancing thermal conductivity of fluids with nanoparticles. In: Siginer DA, Wang HP, editors. Developments and Applications of Non-Newtonian Flows. New York: American Society of Mechanical Engineers. **231**, 99–105.

[14] Chowdhury, R., Parvin, S. and Khan, M.A. (2016). Finite element analysis of double-diffusive natural convection in a porous triangular enclosure filled with Al2O3-water nanofluid in presence of heat generation, Heliyon, **2.**

[15] Devi, M., Gupta, U. and Bandari, S. (2024). Internal heat source effects on thermosolutal convection of Casson nanofluids embedded by Darcy-Brinkman model, Numer HeatTr B-Fund, **85,** 1056-1071.

[16] Dhananjay, Y., Agrawal, G.S. and Bhargava, R. (2011). Rayleigh–Bénard convection in nanofluid, IJAMM, **7**, 61-76.

[17] Huppert, H.E. and Turner, J.S. (1981). Double-diffusive convection., J. Fluid Mech, **106**, 299-329.

[18] Khaled, A.R. and Vafai, K. (2005). Heat transfer enhancement through control of thermal dispersion effects, Int. J. Heat Mass Transfer, **48**, 2172-2185.

[19] Khalid, I.K., Mokhtar, N.F. and Ibrahim, Z.B. (2022). Control effect on Rayleigh-Bénard convection in rotating nanofluids layer with double-diffusive coefficients. CFD Letters. **14**, 79-95.

[20] Khalid, I.K., Mokhtar, N.F., Hashim, I., Ibrahim, Z.B. and Gani, S.S. (2017). Effect of internal heat source on the onset of double-diffusive convection in a rotating nanofluid layer with feedback control strategy, Adv. Math. Phys, **2017**, 2789024.

[21] Khanafer, K., Vafai, K. and Lightstone, M. (2003) Buoyancy-driven heat transfer enhancement in a two-dimensional enclosure utilizing nanofluids, Int. J. Heat Mass Transfer, **46**, 3639-3653.

[22] Kiran, P. and Manjula, S. H. (2023). Internal heat modulation on Darcy convection in a porous media saturated by nanofluid, J. Nanofluids, **12**, 666-675.

[23] Kumari, C., Kumar, J. and Prakash, J. (2024). On the validity of exchange principle in electrothermoconvection in a dielectric fluid saturated densely packed porous medium**,** J. Rajasthan Acad. Phy. Sciences **23**, (1&2) 2024, 14-29.

[24] Kuznetsov, A.V. and Nield, D.A. (2010). Thermal instability in a porous medium saturated by a nanofluid: Brinkman model, Transp. Porous Media, **81**, 409-422.

[25] Lapwood, E.R. (1948). Convection of fluid in a porous medium, Math. Proc. Camb. Philos. Soc., **44**, 508-521.

[26] Malashetty, M.S., Hill, A.A. and Swamy, M. (2012). Double diffusive convection in a viscoelastic fluid-saturated porous layer using a thermal non-equilibrium model, Acta Mech, **223**, 967-983.

[27] Nield, D.A. and Kuznetsov, A.V. (2010). The onset of convection in a horizontal nanofluid layer of finite depth., Eur. J. Mech. B Fluids. **29**, 217-223.

[28] Nield, D.A. and Kuznetsov, A.V. (2009). Thermal instability in a porous medium layer saturated by a nanofluid, Int. J. Heat Mass Transfer, **52**, 5796-5801.

[29] Nield, D.A. and Kuznetsov, A.V. (2012). The onset of double-diffusive convection in a nanofluid layer, Int. J. Heat Fluid Flow, **32**, 771-776.

[30] Nield, D.A. and Kuznetsov, A.V. (2014). The onset of convection in an internally heated nanofluid layer, J. Heat Transf, **136**, 014501.

[31] Prakash, J. and Bala, R. (2016). On arresting the complex growth rates in ferromagnetic convection with magnetic field dependent viscosity in a rotating sparsely distributed porous medium, J. Appl. Mech. Tech. Phys., **57**(4), 623-636.

[32] Pundir, S.K., Awasthi, M.K. and Kumar, V. (2020). Double-diffusive convection in a hybrid nanofluid layer, J. Nanofluids, **11**, 296-304.

[33] Radko, T. (2003). A mechanism for layer formation in a double-diffusive fluid, J. Fluid Mech., **497,** 365-380.

[34] Sharma, J. and Gupta, U. (2015). Double-diffusive nanofluid convection in porous medium with rotation: Darcy-Brinkman model, Procedia Eng, **127,** 783-790.

[35] Turner, J.S. (1974). Double-diffusive phenomenon. Annu. Rev. Fluid Mech., **6**, 37-56.

[36] Tzou, D.Y. (2008). Thermal instability of nanofluids in natural convection, Int. J. Heat Mass Transfer, **51**, 2967-2979.

[37] Umavathi, J.C. and Bég, O.A. (2020). Modeling the onset of thermosolutal convective instability in a non-Newtonian nanofluid-saturated porous medium layer, Chin. J. Phys, **68**,147-167.

[38] Wong, K.V. and De Leon, O. (2010). Applications of nanofluids: current and future, Adv. Mech. Eng. **2**, 519659.

[39] Yadav, D., Agrawal, G.S. and Bhargava, R. (2011). Thermal instability of rotating nanofluid layer, Int. J. Eng. Sci, **49,** 1171-1184.

[40] Yadav, D., Agrawal, G.S., Bhargava, R. (2013). Onset of double-diffusive nanofluid convection in a layer of saturated porous medium with thermal conductivity and viscosity variation, J. Porous Media, **16**, 105-121.

[41] Yadav, D., Bhargava, R. and Agrawal, G.S. (2012). Boundary and internal heat source effects on the onset of Darcy–Brinkman convection in a porous layer saturated by nanofluid, Int. J. Therm. Sci, **60**, 244-254.